Front. Phys. 11(2), 117803 (2016)
DOI 10.1007/s11467-015-0490-0

REVIEW ARTICLE

Single-site surface-enhanced Raman scattering beyond spectroscopy

Mai Takase[†], Satoshi Yasuda, Kei Murakoshi[‡]

Department of Chemistry, Faculty of Science, Hokkaido University, Sapporo, Hokkaido 060-0810, Japan

Corresponding author. E-mail: [‡]kei@sci.hokudai.ac.jp

Received November 3, 2015; accepted November 20, 2015

Recent progress in the observation of surface-enhanced Raman scattering (SERS) is reviewed to examine the possibility of finding a novel route for the effective photoexcitation of materials. The importance of well-controlled SERS experiments on a single molecule at a single site is discussed based on the difference in the information obtained from ensemble SERS measurements using multiple active sites with an uncontrolled number of molecules. A single-molecule SERS observation performed at a mechanically controllable breaking junction with a simultaneous conductivity measurement provides clear evidence of the drastic changes both in the intensity and in the Raman mode selectivity of the electromagnetic field generated by localized surface plasmon resonance. Careful control of the field at a few-nanometer-wide gap of a metal nanodimer results in the modification of the selection rule of electronic excitation of an isolated single-walled carbon nanotube. The examples shown in this review suggest that a single-site SERS observation could be used as a novel tool to find, develop, and implement applications of plasmon-induced photoexcitation of materials.

Keywords surface-enhanced Raman scattering, localized surface plasmon resonance, metal nanostructure, single-molecule observation, single-walled carbon nanotube, selection rule of electronic excitation

PACS numbers 78.30.-j, 73.20.Mf, 71.45.Gm, 33.20.Kf

Contents

1 Introduction

Notably, an intrinsic limit to the interaction between matter and light exists [1]. Generally, the limit is characterized by the value of the photon-absorption cross sections, as at least 10^7 molecules are required to catch a single photon, even in molecules showing strong light-absorption properties. The ability to modify the light-matter interaction can lead to the fabrication of more effective photoenergy conversion devices. Recently, plasmonics has been developed as a novel way to control light [2, 3]. The photoillumination of a small metal nanostructure results in the excitation of a localized surface plasmon resonance (LSPR). The resonant oscillation of the free electrons, due to the excitation of the LSPR, generates a confined electromagnetic field in the vicinity of the structure. The energy and the polarization direction of the field are tailored by controlling the size and anisotropy of the metal nanostructure. Highly confined fields at the interfaces of metals and dielectrics can provide small and slow light effects.

The positioning of matter in this field results in an apparent modification of the interaction between matter and light, compared with the general situation observed under light illumination of matter [4]. A highly localized field generates a huge gradient of field intensity over a distance smaller than 10 nm. Generally, the interac-

*Special Topic: Frontiers of Plasmonics (Ed. Hong-Xing Xu).
[†]Present address: Graduate School of Engineering, Muroran Institute of Technology, Muroran, 050-8585, Japan

tion between matter and light is defined by a situation in which the electronic structure is uniformly polarized at the scale corresponding to the light wavelength, e.g., hundreds or a thousand nm for visible to infrared light. Upon excitation of matter by the LSPR, this approximation may fail, leading to a change in the optical properties. Although this change has been pointed out for systems showing vibrational symmetry [5], experimental proof of the electronic excitation has not been obtained, owing to the difficulties to prepare an appropriate nanosystem, as well as the observation itself.

To investigate the change in the optical response of the matter in the LSPR field, surface-enhanced Raman scattering (SERS) measurements can be quite useful. From the discovery of the SERS phenomenon, the observations have provided fruitful information on the optical response of matter in the LSPR field, such as characteristic absorption, emission, and electronic and vibrational excitations [6–8]. The established SERS model explains the apparent enhancement factor of the SERS signal by considering the intensity of the localized electromagnetic field. An additional enhancement due to electronic excitation resonance at the interfaces between molecules and metal surfaces is known to be an additional important factor [9, 10]. Despite active studies on SERS for more than 40 years, however, unsolved issues still remain in clarifying the mechanism of the SERS phenomenon observed in systems exhibiting an extremely strong enhancement. A very specific molecular dependence on SERS implies that characteristic changes in the optical responses of molecules in LSPR fields could be monitored.

In this review, recent progresses in SERS observations to clarify the mechanism of enhancement are briefly summarized. After a discussion on the importance of single-molecule observations, the information obtained from observed SERS spectra is discussed. Several observations seem to provide unique experimental evidence of the change in the optical responses of molecules in the LSPR field. After a summary of the interpretations of the phenomenon, the expectations on further developments of the systems are discussed in relation to the use of the LSPR field as a source of effective excitation of materials.

2 Single-site SERS for single-molecule observation

From the very early stages of the study of SERS, single-molecule sensitivity has been under intense discussion. Although several behaviors of the SERS signals, such as blinking, fluctuation, specific Raman mode selectivity, etc., had been regarded as proofs of single-molecule SERS observations, a considerably clearer evidence of the experimental observation was still required to obtain characteristic information on a single molecule [7, 11, 12].

Despite the strong requirements for the evidence of single-molecule observation, experimental difficulties to define the number of target molecules as well as the metal nanostructures for light confinement still exist as unsolved issues, hindering a deeper understanding of the SERS phenomenon. Controlling the number of molecules on metal surfaces is particularly difficult. In the early stages of SERS, most studies tried to control the number of molecules through the introduction of an ultra-low concentration of molecules [12]. Although the estimation of the number of molecules by assuming the average density of the observation area, e.g., 1 μm^2 scale for a confocal microscope spot, could be used, additional proof is indispensable to exclude the effect of aggregation due to an inhomogeneous distribution, which leads to inaccuracy in the single-molecule observation. The importance of the diffusion of adsorbed or dissoluble molecule in two or three dimensions has been actually well recognized. The control of the number of molecules in the observation area is a critical factor, especially for a system with thermal fluctuations at room temperature.

The difficulties associated with molecule control were solved by the introduction of a two-analyte technique [13–17]. An ensemble SERS measurement using multiple SERS active sites with aggregates of a target molecule often provides time- and space-averaged information on molecules, such as composition, structures, and orientation on the surface. Averaged information on molecules is sometimes the same as that obtained by ordinary spectroscopic methods, with relatively low sensitivity, using a sufficient amount of target molecules. In the case of the two-analyte technique, the introduction of two SERS-active analytes into a SERS observation provides information on the respective analyte molecules under observation [13, 16]. As the absolute number of molecules in the microscopic SERS observation area decreases, the probability of observation on the SERS spectrum of only one of the two analytes increases. A single-molecule observation can be obtained if the two analytes are distributed homogenously without aggregation. The validity of the idea was confirmed by the use of different isotopologues adsorbed onto aggregates of metal nanoparticles to monitor the SERS two-dimensional (2D) correlation [17]. In a system with low coverage, only one type of isotope-labeled molecule was observed, showing the probability with a combined Poissonian binomial distribution. The result is also regarded as a strong proof of

single-molecule SERS observation.

A well-controlled number of molecule systems for the two-analyte SERS observation provide additional information on the SERS active site, showing enormous enhancement. The number of molecules observed by SERS is defined via controlled adsorption at the liquid/solid interface under adsorption-desorption equilibrium. The adsorption isotherm gives information on the number from the coverage of the target molecule. The two-analyte SERS experiment performed with a relatively low concentration solution (1 μM) provides only a single analyte spectrum at the gap of a metal nanodimer [16]. The puzzling question comes from the value of the estimated coverage of the target molecule on the surface. At that concentration, the coverage of observed molecules is 0.2–0.3 monolayer, according to previously documented values from the isotherm [18, 19]. The result of the two-analyte experiment, in which only one of two analytes is observed, implies that the size of the SERS active site is comparable with that of a single-molecule adsorption site, despite the fact that finite-difference time-domain calculations show that the area of the localized electromagnetic field is in the range of a few to tens of square nanometers [20]. Not only the two-analyte technique confirms the single-molecule SERS observation, but it also proves the existence of molecule-size SERS active sites at a scale far below the localization of the electromagnetic LSPR field.

In addition to the number of molecules, the control of the spatial distribution of the localized electromagnetic field is another important factor to realize site-selective observation of a single target molecule. Thus, the use of a metal sharp tip with the scanning microscopy technique for SERS, named tip-enhanced Raman scattering (TERS), has been developed to control the localization of the field. After the findings regarding the modification of the fluorescence lifetime of molecules in the vicinity of a scanning probe microscope tip [21], a specially resolved TERS observation was developed [3, 22]. The lateral resolution drastically improved from <100 nm of the initial studies down to the current single-molecule scale [23, 24]. Developed techniques have been applied not only to single-molecule imaging [25], but also to the investigation of the phonon structure of an ultrasmall crystalline boundary [26], single-molecule switching [27], distribution of the electromagnetic field of a single metal nanorod, [28] and dynamics of vibration in an ultrashort timescale [29]. In a well-controlled ultrahigh vacuum environment at low temperature ($<10^{-8}$ Pa, <80 K), TERS was used for the imaging of the inner structure of a single molecule via the matching of the resonance of the nanocavity plasmon to the molecular vibronic transitions (Fig. 1) [25, 30]. A well-resolved Raman image of a single molecule obtained by TERS gives insight into the interaction between molecules and LSPR field. A successful TERS observation, however, maintains several unsolved questions regarding the image. A highly confined electromagnetic field generates a huge gradient of field intensity, which may affect the spatial resolution and selection rule for the detection of specific vibrational modes [31]. The contribution of the field gradient on a TERS image is still under discussion [32]. The interpretation of the observed enhanced Raman spectrum with TERS requires further careful considerations on the interaction between the molecule and the LSPR field to determine the chemical structure, orientation, excited states of electrons, and vibrations of the molecule on the surface, even when the interaction with the surface is relatively weak [33]. To apply the technique to systems at room temperature in various environments, such as electrolyte solutions, gas mixtures, and phase-separated crystallites to understand the chemistry, additional ideas seem to be required.

3 Simultaneous observation of SERS and conductivity of a single-molecule junction

Additional information on the properties or functionalities of an isolated single molecule is needed to fully understand the observed single-molecule SERS spectrum. An interesting property of a single molecule is its conductivity [34]. Single-molecule junctions composed of a metal-molecule-metal motif have been widely investigated with the aim to realize molecule-scale components for novel electronic devices, in the future. Not only electronic transport, but also the responses of mechanics, thermoelectrics, optoelectronics, and spintronics properties have been examined to construct ultrasmall logic gates [35]. Recent efforts have been focused on the precise control of the functions of a single-molecule junction.

The control of the electronic transport is the key to realizing the devices. The choice of the molecules is the most important, as the characteristics of the electronic structure, such as the electrochemical potential of electrons in molecular orbitals determine the electron transport properties [36, 37]. Although the states are defined by the molecule structure [38], the electronic structure is also affected by the strength of the adsorption onto metals [39]. Photoexcitation could also alter the potential of the molecular orbitals [40]. The simultaneous observation of SERS with a conductivity measurement could provide the key role of the electronic states, which can control the conductivity by changing the orientation of

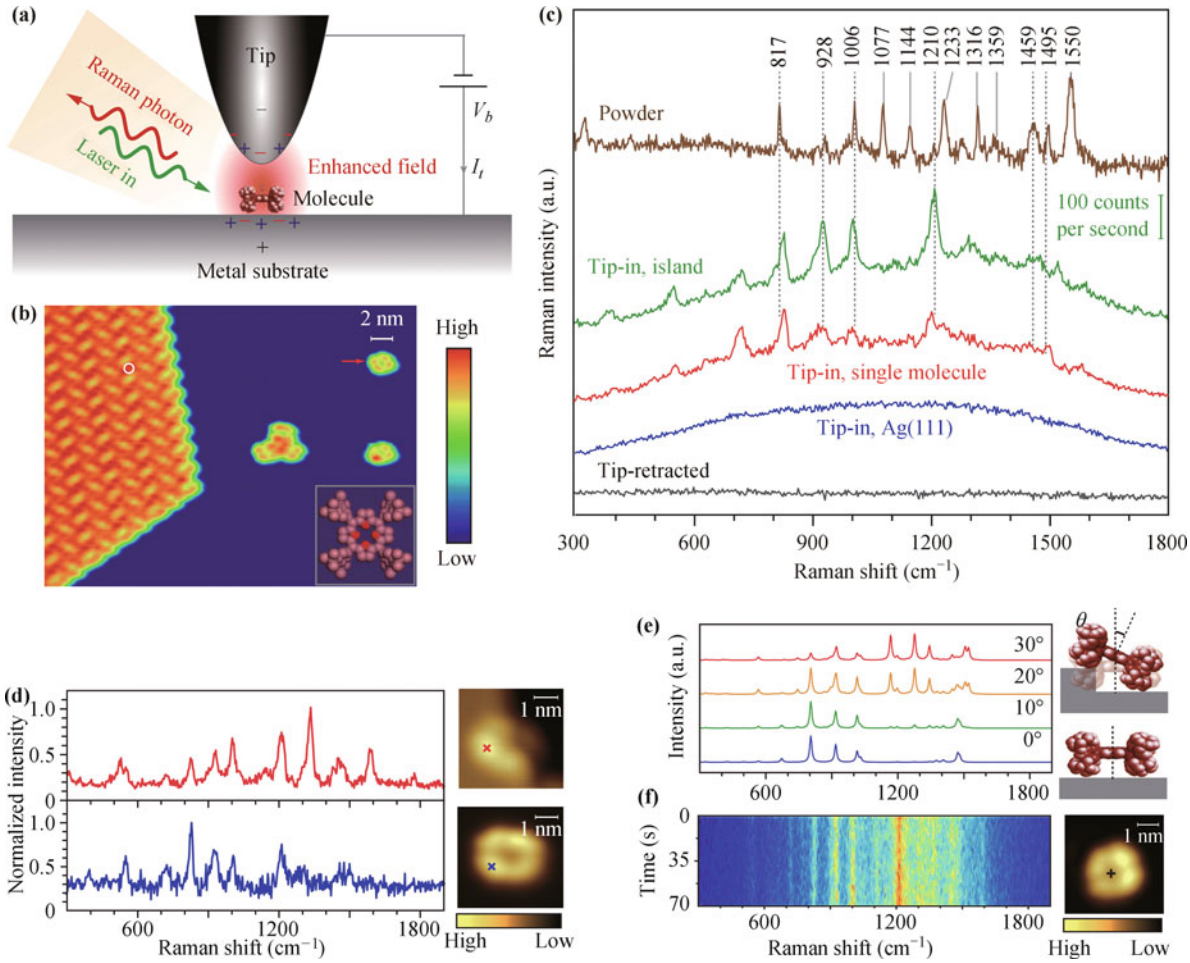

Fig. 1 **(a)** Schematic tunnelling-controlled TERS in a confocal-type side-illumination configuration, in which V_b is the sample bias and I_t is the tunnelling current; **(b)** STM topograph of sub-monolayered H2TBPP molecules on Ag(111) (1.5 V, 30 pA, 35 nm×27 nm). The inset shows the chemical structure of H2TBPP and the white circle indicates one representative site for TERS measurements on the molecular islan; **(c)** TERS spectra for different conditions. The tip-in spectra were acquired at 120 mV, 0.5 nA and 3 s. The green spectrum is taken on top of the molecular island (the green scale bar shows the signal level detected by charge-coupled device (CCD). The red spectrum is taken on top of a single molecule (marked by the red arrow in b). The blue spectrum is taken on bare Ag(111). The black spectrum is taken on top of the molecular island but with the tip retracted 5 nm from the surface (120 mV, 3 s). For comparison, a standard Raman spectrum (*brown*) is shown on the top for a powder sample of H2TBPP molecules; **(d)** Single-molecule TERS spectra (100 mV, 1 nA, 3 s) for an isolated H2TBPP molecule adsorbed on the terrace (bottom, *blue*) or at the step edge (top, *red*) of Ag(111). Both spectra were acquired on the molecular lobes marked with crosses in the STM images on the right (subtracted from the broad continuum for clarity); **(e)** Calculated TERS spectra of a molecule for different tilt angles θ. Shown on the right are the schematics of flat-lying and tilted molecules, respectively; **(f)** 35 sequential TERS spectra (120 mV, 1 nA, 2 s) acquired on the centre of a single flat-lying H2TBPP molecule adsorbed on the Ag(111) terrace (the terrace is the flat area between the step edges); the centre is marked as a cross in the corresponding STM image on the right. Reproduced with permission from Ref. [25], Copyright © 2013 Macmillan Publishers Ltd.: Nature.

a single molecule under photoillumination and current flow.

The mechanically controllable break junction (MCBJ) technique has been used for simultaneous measurements of SERS and conductivity [41–45]. Although the scanning probe technique is also available to characterize single-molecule junctions, this method is often suitable for high-speed conductance dynamics characterization during the breaking junction [27]. The MCBJ technique is able to maintain the structure of a single-molecule junction as relatively stable. Typically, single-molecule SERS measurements require an exposure time of spectral accumulation of at least a few hundred milliseconds. The correlation between SERS spectrum and conductivity changes depending on the time. A fluctuating conductance gives a complex change in the SERS spectrum, causing difficulties in the determination of the physical origin of the intensity change of specific Raman modes. Although the origins of the correlation between the conductance and the spectrum have been attributed to the

photon-driven charge excitation of the electronic states at the molecule and metal surfaces [40], and to the contribution of dark multipolar modes of LSPR at the metal nanogap [43], a thorough explanation of the SERS spectrum change at a single-molecule junction has not been provided. In MCBJ systems, the control of a single molecule to fabricate a stable junction is also indispensable to discuss the correlation with conductivity.

The application of the MCBJ technique to a system in adsorption/desorption equilibrium is also valuable to control the interaction between molecule and metal, as in the case of a metal nanodimer for a single-site molecule SERS measurement. A single-molecule MCBJ in equilibrium results in the formation of a single-molecule bridge with a relatively high stability, typically kept for a period ranging from a few to a few tens of milliseconds, even at room temperature in a solution [46–48]. During the formation of a single-molecule bridge confirmed by the conductivity, the characteristic evolution of the intense Raman bands is observed (Fig. 2) [44]. The observed bands are assigned to the non-totally symmetric modes, b_1 and b_2, of the molecule, which are not observed before or after the formation of a single-molecule bridge. The frequency of the observation, as well as the observed strong band intensities of the non-totally symmetric modes, is well correlated with the conductivity. The observed non-totally symmetric modes could be explained by an additional polarization molecule via electronic excitation. The process is proposed as a charge transfer process that induces vibronic coupling, as in the case of a SERS observation at a roughened electrode [49]. Considering the correlation between the conductivity and observed intensity of the b_1 and b_2 modes, the observation of the b_2 mode reflects a strong binding of the molecule to the surface of the metal with the orientation parallel to the direction of the electromagnetic LSPR field. A conductivity fluctuation is also well correlated with the formation of the strong binding of a single molecule by the b_2 mode observation. By using the system in equilibrium, the self-organized formation of a single-molecule junction at room temperature in a solution is successfully confirmed by the simultaneous measurement of SERS and conductivity.

The observation of the non-totally symmetric mode showing relatively intense scattering implies the additional effect of the optical excitation of the electronic states by the LSPR field. In the system of a single-molecule bridge, the symmetry of the molecule orbitals contributing to the electronic excitation predicts a relatively weak interaction with the LSPR field [44]. The increased scattering intensity of the non-totally symmetric mode needs further explanation for the effective resonance process due to the excitation [44]. The possibility of the modulation of the selection rules of the optical absorption process at a highly localized electromagnetic field with a steep gradient of the field intensity has been pointed out [3]. This effect could contribute to increments in the scattering intensity of the non-totally symmetric mode of the system. A very strong intensity of a single-molecule SERS of a specific mode at the MCBJ could reflect not only the orientation of the molecule, but also the characteristic photoresponse of the molecule in the LSPR field.

4 Exotic electronic excitation of matter by confined photons

The improvement of a single-site SERS experiment for a single molecule leads to the possible observation of the modulation of the photoexcitation process in the LSPR field. Generally, the selection rules of photoexcitation assume the long wavelength approximation, indicating that the field amplitude is assumed constant and uniform within a molecule. The LSPR field, however, has a significantly high intensity gradient. In a field with such an extreme gradient at the molecular scale, the conventional limitations of the optical response are expected to be violated (Fig. 3) [50]. Although the effects of the field gradient on the selection rules of vibrational excitations have been well studied both in theory [5, 51, 52] and through experiments [53], those of electronic excitation have not yet been confirmed experimentally. The change in the selection rules of electronic excitation by LSPR can be crucial to understand single-molecule SERS.

As a molecule target, an isolated single-walled carbon nanotube (SWNT) is one of the most suitable choices because of the well-defined electronic states characterized by van Hove singularities due to 2D quantization. The anisotropic tube structure is also an advantage to detect the direction of a highly oriented LSPR field. SERS observation of SWNTs has been an active field [54–58]. After an innovative SERS work confirming the changes in the Raman scattering tensor by the large field gradients generated by aggregated Ag particles on multiple SWNTs [55], SERS observations of an isolated SWNT have been well developed. Despite the development of the observation techniques of an isolated SWNT [57], the change in the selection rules has not yet been confirmed.

An isolated SWNT is placed in the nanogap of a metal nanodimer, showing the SERS spectral profile of the G band modes consisting of the $A^{\pm}$, $E_1^{\pm}$, and $E_2^{\pm}$ modes (Fig. 4) [59], reflecting the title angle of the tube axis

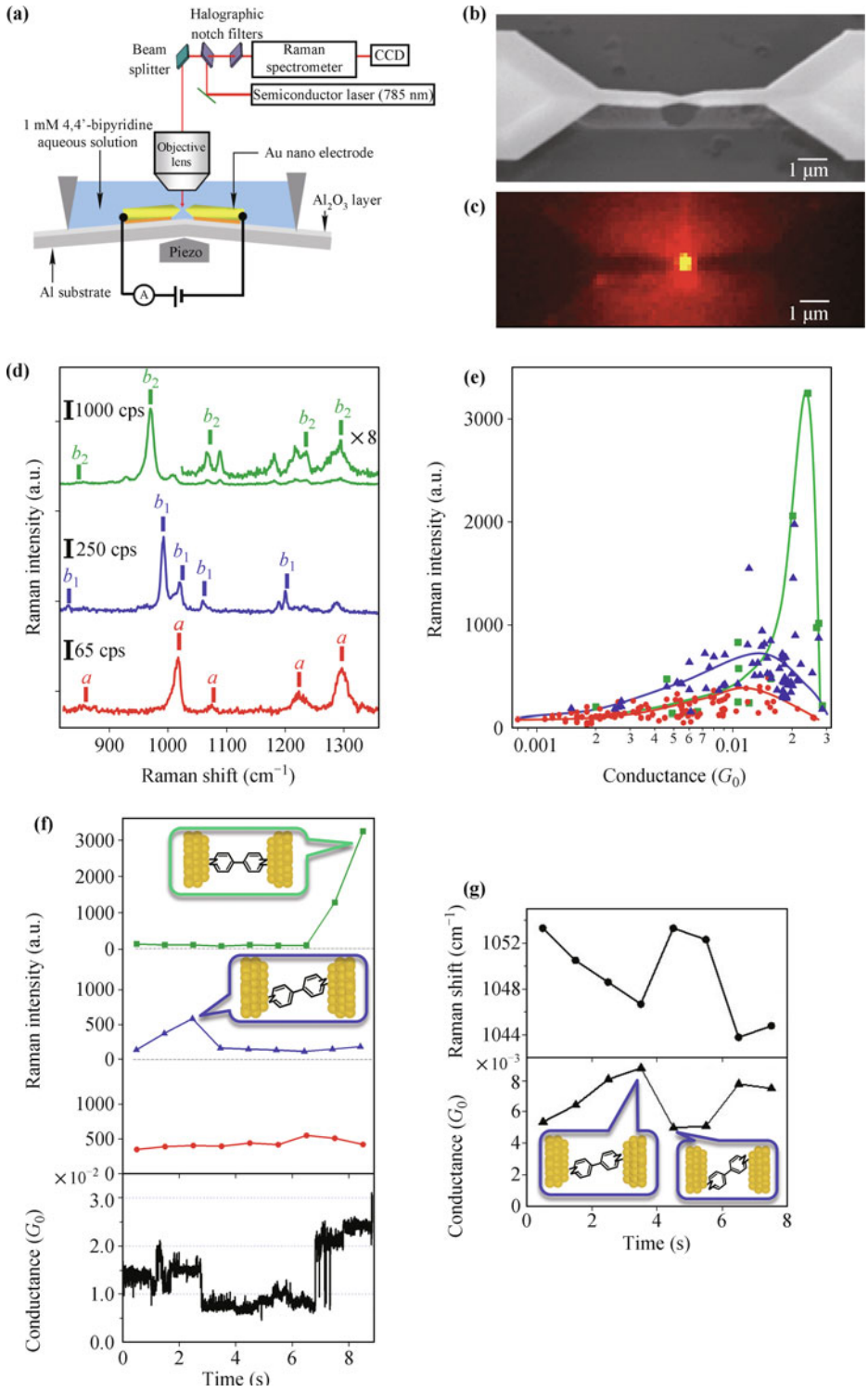

Fig. 2 **(a)** Schematic view of the MCBJ-SERS system; **(b)** SEM image of an Au nanobridge in the MCBJ sample; **(c)** Raman imaging of the Au nanogap observed at 1015 cm^{-1}; **(d)** Three types of SERS spectra of a single 4,4'-bipyridine molecule junction. Assignment of the totally symmetric *a* mode (*red*), and the nontotally symmetric b_1 mode (*blue*) and b_2 mode (*green*) are shown as dotted lines; **(e)** SERS intensity dependence of a (*red*), b_1 (*blue*), and b_2 (*green*) modes on the conductance of the junction; **(f)** Time course of the Raman intensity of the *a* mode (*red*), b_1 mode (*blue*), and b_2 mode (*green*) together with the conductance of the molecular junction; **(g)** Time course of the energy of the b_1 mode of the ring breathing around 1050 cm^{-1} and the conductance of the single molecule junction. Schematics of the relevant molecular orientation are shown as insets. Reproduced in part with permission from Ref. [44], Copyright © 2013 American Chemical Society.

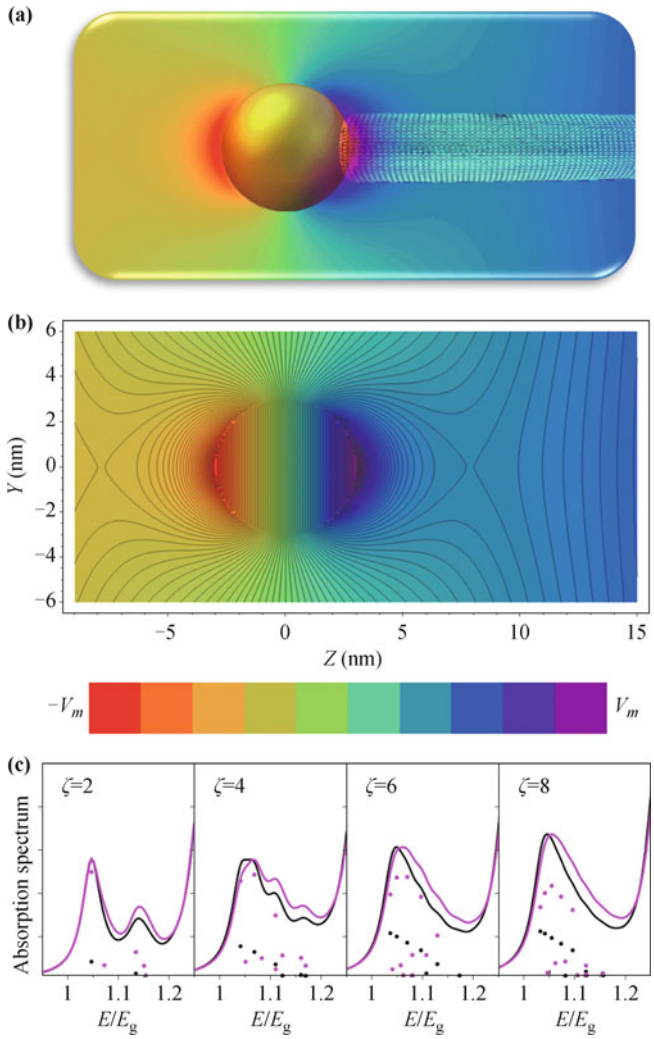

Fig. 3 **(a)** Schematic illustration of the geometry of a metal-tipped nanorod used to model the effect of a near-field on the optical transitions of a nanoscale system; **(b)** Isopotential contour lines of the near-field potential generated by a gold nanoparticle of 6 nm diameter. V_m is the maximal potential on the surface of the gold nanoparticle; **(c)** The absorption rates in CdSe (left) and CdS (right) 20 nm nanorods of aspect ratio $7^{1/2}$. The lines represent results for different metal tip diameters ranging from zero (*black*) to 10 nm (*magenta*) in steps of 2 nm. The relative oscillator strengths for the strongest transitions are shown for individual transitions for the smallest and largest metal tip sizes. Inset: The absorption maximum (*blue*) shift as a function of metal tip diameter. Solid and dashed lines correspond to CdSe and CdS, respectively. Reproduced from Ref. [50].

with respect to the long axis of the nanodimer [56]. The simultaneous observation of the radial-breathing mode (RBM) confirms the observation of an isolated SWNT. In the case of the successful preparation of highly dispersed SWNTs onto a metal nanodimer with a gap of 1–2 nm, the SERS spectrum of the SWNT via the resonance of the E_{14} transition is normally forbidden. A newly developed theoretical method to calculate the optical response is the extended discrete dipole approximation (EDDA), wherein the nonlocal response within a single molecule can be treated by including the nanoscale spatial interplay between the electric field and molecular wave functions. By combining this method with the newly developed theory to calculate electronic states of SWNTs (including the dynamic e-h exchange interaction), we calculated the optical signal for several transitions. As a result, the observed data certainly included the signal corresponding to a calculated one showing the optical forbidden transition. In this case, a highly localized electric field at the nanogap induces a transition that is forbidden under the usual long wavelength approximation conditions. The origin of the phenomenon can be interpreted as a huge gradient within a 1-nm-wide space, where a quadruple transition is dominant (Fig. 5).

There is a possibility of controlling the optical electronic transitions of a SWNT by using metal nanodimers with a controlled nanogap distance. The highly systematic identification of the excitations of individual

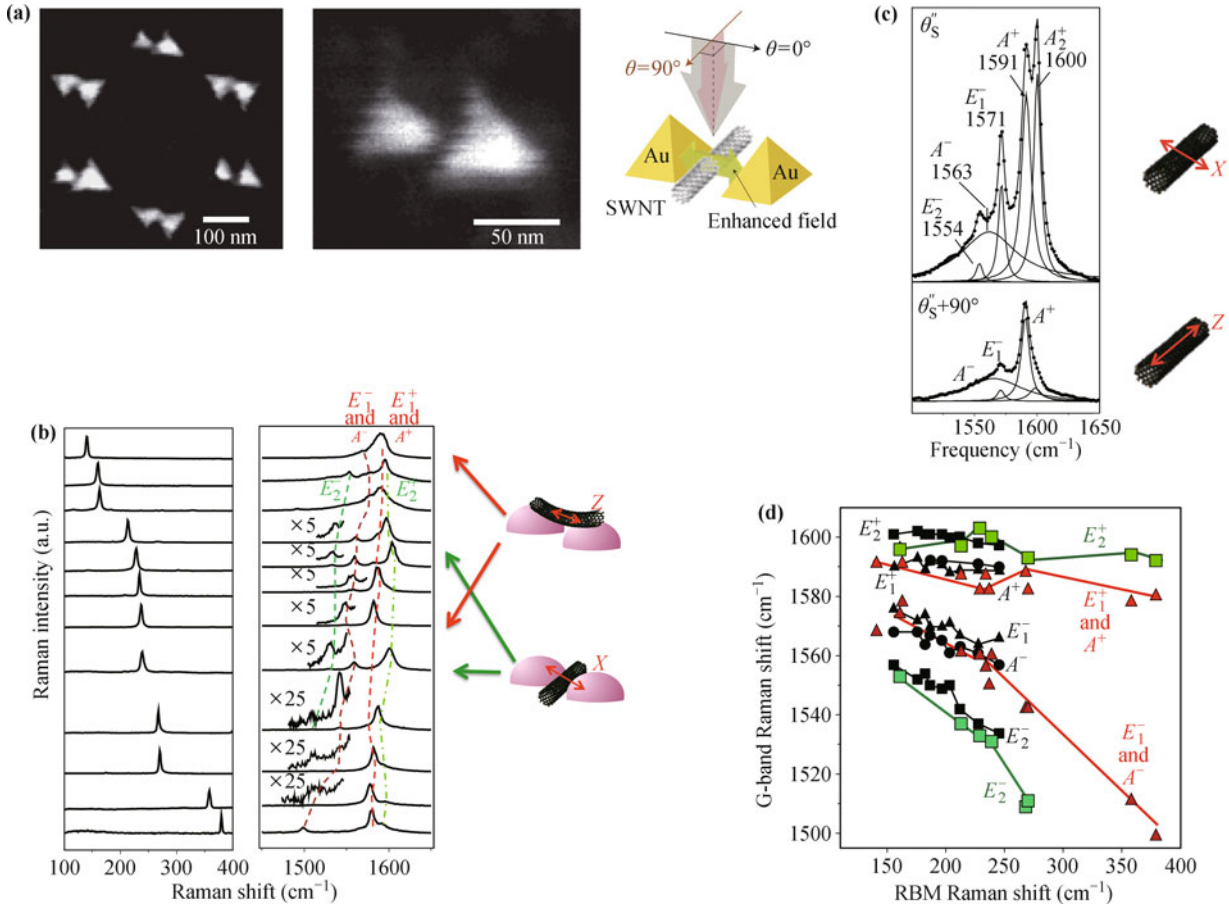

Fig. 4 **(a)** SEM images of well-defined gold nanodimers and illustration of an SWNT lying in the nanogap of a dimer and the enhanced field polarization; **(b)** Representative SERS spectra of individual SWNTs observed with incident light polarized parallel to the long axis of the nanodimer [59]; **(c)** Polarization scattering geometry dependence for G band from isolated SWNTs. Reproduced in part with permission from Ref. [56], Copyright © 2003 American Physical Society. **(d)** Diameter dependent changes of G band frequencies relative to RBM frequencies. (a, b, d) Reproduced in part with permission from Ref. [59], Copyright © 2013 Macmillan Publishers Ltd.: Nature Photonics.

SWNTs through well-resolved Raman signals implies a breakdown of the selection rules, due to the strong field gradient in the radial direction of the SWNTs (Fig. 5) [60]. Although the break in the selection rule of the electronic excitation in a nanostructured electric field whose size is comparable with those of the molecules has been discussed in photochemistry text books as challenging problem [1], few experimental reports have been provided until now. Clearly, a careful determination of the angle between a SWNT and the LSPR field at a single site is indispensable for the observation. Notably, an insufficient conformation to the direction at the isolation of a SWNT at a metal nanogap leads to a failure in the observation of polarization-dependent selective G band modes, as well as to the wrong discussion for the assignment [61].

The importance of the change in the selection rules has been recognized, especially in the field of nanophotonics. Achieving an optical response beyond the conventional selection rule should alter both the quantum efficiency and energy of electrons and holes in materials [62]. The applications should not be limited to spectroscopy, but also include a variety of research fields, such as photochemistry, solid-state photophysics, photobiology, etc. in which effective photoexcitation is required. The use of SERS has been shown to be quite effective to explore a novel route for photoexcitation in nanomaterials with desired photofunctions.

5 Future expectations

A single-site SERS observation of a single molecule pro vides useful information on molecules and nanomaterials in the LSPR field. The SERS phenomenon is still partly unsolved for the practical application of an ultrasensitive detection, as well as a quantitative analysis of multianalyte samples. A principle to uncover the unexpected

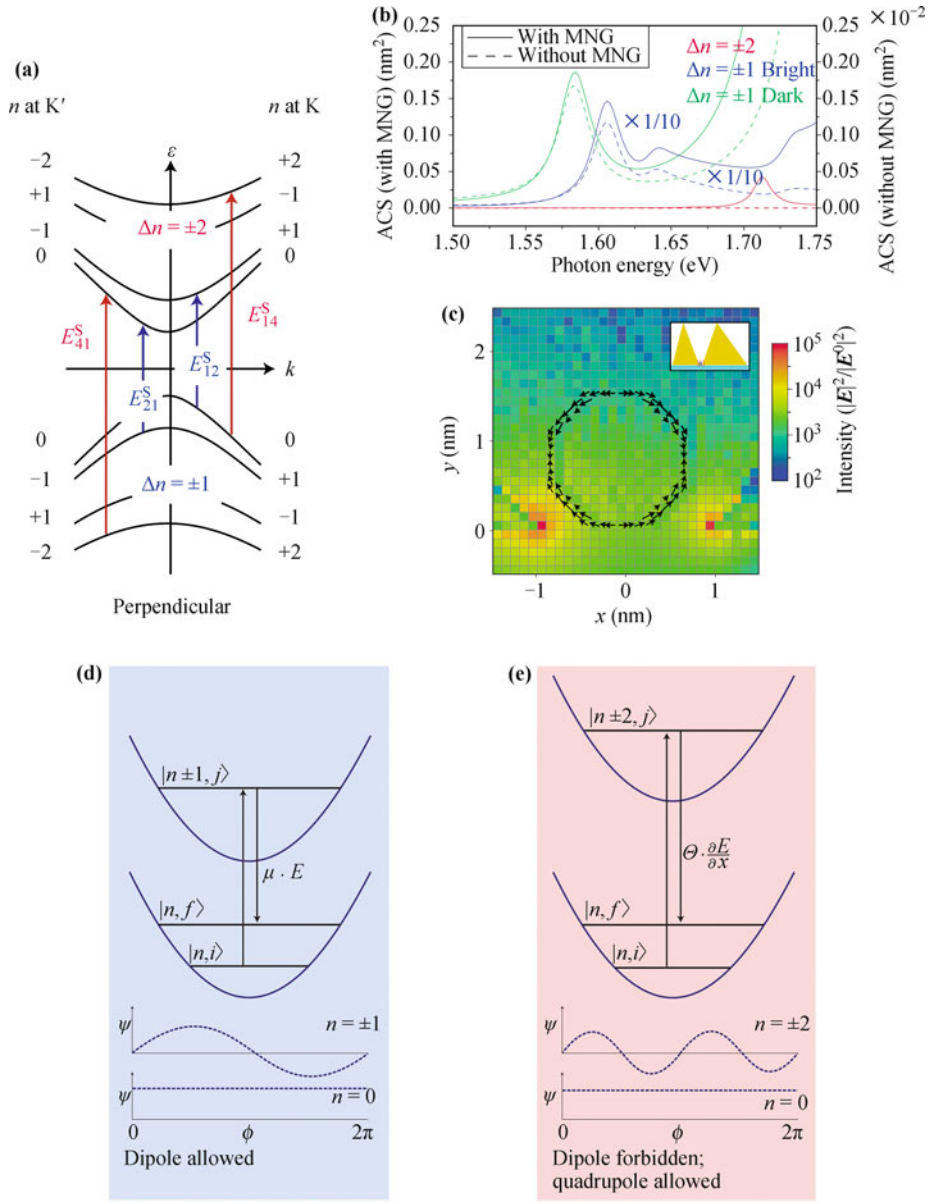

Fig. 5 **(a)** Energy bands and optical transitions of a semiconducting SWNT; **(b)** Selection-rule breakdown as revealed by an EDDA calculation; Absorption cross-section (ACS) with (solid lines, left-hand scale) and without (dotted lines, right-hand scale) the metallic nanogap (MNG), as given by the EDDA calculation. Results indicated by the solid and dotted blue lines are reduced by a factor of 10. **(c)** Cross-sectional view of the calculated intensity of the EM field, which includes both the longitudinal and transverse components, under resonant excitation conditions of the E_{14} exciton. The calculated quadrupole polarization of the E_{14} exciton is also shown by black arrows. The grids show the cell size in the present DDA calculation. Reproduced in part with permission from Ref. [59], Copyright © 2013 Macmillan Publishers Ltd.: Nature Photonics. **(d, e)** Important electronic transitions for resonance Raman spectroscopy; For the particle-in-ring model, the $\Delta n = \pm 1$ transition has a nonzero dipole transition moment μ, which couples to the field E to give resonance Raman scattering. The $\Delta n = \pm 2$ transition has a nonzero quadrupole transition moment Θ, which couples to the field gradient to give resonance Raman scattering. At the bottom of each panel, representative wavefunctions associated with the particle-in-ring model for $n = 0, \pm 1, \pm 2$ are depicted. Multiplying these by $\mu \approx \sin\phi$ and $\Theta \approx \sin 2\phi$ shows why the ± 1 transition is dipole allowed, whereas the ± 2 transition is quadrupole allowed. Reproduced in part with permission from Ref. [59], Copyright © 2013 Macmillan Publishers Ltd.: Nature Photonics.

selectivity of molecules seems still unclear. However, the exotic behavior of a vibrational spectrum at a single-site SERS for single-molecule measurement implies that the responses can be used to understand the unusual photoexcitation process of nanomaterials in the LSPR field. Recent intensive studies for nanoplasmonics apparently show the importance of quantum photonics at the atomic scale for a charge transfer plasmon [63], ultrasmall con-

fined optical cavity [64–66], coherence of excitons with photons [67], etc. Highly confined fields proposed in these advanced studies could be applied to establish novel selection rules of the electronic excitation in the LSPR field, leading to the generation of excited electrons and holes with distinct electrochemical potentials in materials. In the field of chemistry, modifying electronic excitation by light leads to changes in the framework of photoenergy conversion [4]. Although the control of the photoexcitation process has not been achieved yet, the investigation of single-site SERS provides abilities beyond ultrasensitive spectroscopy to explore novel systems with advanced photofunctionalities.

Acknowledgements The authors are grateful to Profs. Hong-Xing Xu, Zhong-Qun Tian, Peter Nordlander, Javier Aizpurua, and Toshiharu Teranishi for helpful discussions. This work was partially supported by Grants-in-Aid for scientific research from the Ministry of Education, Science and Culture, Japan (Grant Nos. 26248001, 26620188, and 25620003), and the Canon Foundation.

References

1. N. J. Turro, V. Ramamurthy, and J. C. Scaiano, Transitions Between States: Photophysical Processes, Modern Molecular Photochemistry of Organic Molecules, University Science Books, 2010, pp 109–167
2. A. F. Koenderink, A. Alù, and A. Polman, Nanophotonics: Shrinking light-based technology, *Science* 348(6234), 516 (2015)
3. A. M. Kern, D. Zhang, M. Brecht, A. I. Chizhik, A. V. Failla, F. Wackenhut, and A. J. Meixner, Enhanced single-molecule spectroscopy in highly confined optical fields: From $\lambda/2$-Fabry–Pérot resonators to plasmonic nano-antennas, *Chem. Soc. Rev.* 43(4), 1263 (2014)
4. H. Nabika, M. Takase, F. Nagasawa, and K. Murakoshi, Toward plasmon-induced photoexcitation of molecules, *J. Phys. Chem. Lett.* 1(16), 2470 (2010)
5. G. S. Kedziora and G. C. Schatz, Calculating dipole and quadrupole polarizabilities relevant to surface enhanced Raman spectroscopy, *Spectrochim. Acta Part A* 55, 625 (1999)
6. L. E. C. Ru and P. G. Etchegoin, Transitions between states: Photophysical processes, principles of surface-enhanced Raman spectroscopy and related plasmonic effects, Elsevier Science, 2008
7. Y. S. Yamamoto, Y. Ozaki, and T. Itoh, Recent progress and frontiers in the electromagnetic mechanism of surface-enhanced Raman scattering, *J. Photochem. Photobiol. Photochem. Rev.* 21, 81 (2014)
8. Y. S. Yamamoto, M. Ishikawa, Y. Ozaki, and T. Itoh, Fundamental studies on enhancement and blinking mechanism of surface-enhanced Raman scattering (SERS) and basic applications of SERS biological sensing, *Front. Phys.* 9(1), 31 (2014)
9. J. R. Lombardi, R. L. Birke, T. H. Lu, and J. Xu, Charge-transfer theory of surface enhanced Raman-spectroscopy — Herzberg–Teller contributions, *J. Chem. Phys.* 84(8), 4174 (1986)
10. R. L. Birke, V. Znamenskiy, and J. R. Lombardi, A charge-transfer surface enhanced Raman scattering model from time-dependent density functional theory calculations on a Ag-10-pyridine complex, *J. Chem. Phys.* 132(21), 214707 (2010)
11. K. Kneipp, G. Harrison, S. Emory, and S. Nie, Single-molecule Raman spectroscopy: Fact or fiction? *Chimia* 53, 35 (1999)
12. P. G. Etchegoin and E. C. Le Ru, A perspective on single molecule SERS: Current status and future challenges, *Phys. Chem. Chem. Phys.* 10(40), 6079 (2008)
13. E. C. Le Ru, M. Meyer, and P. G. Etchegoin, Proof of single-molecule sensitivity in surface enhanced Raman scattering (SERS) by means of a two-analyte technique, *J. Phys. Chem. B* 110(4), 1944 (2006)
14. E. Blackie, E. C. Le Ru, M. Meyer, M. Timmer, B. Burkett, P. Northcote, and P. G. Etchegoin, Bi-analyte SERS with isotopically edited dyes, *Phys. Chem. Chem. Phys.* 10, 4147 (2008)
15. E. J. Blackie, E. C. Le Ru, and P. G. Etchegoin, Single-molecule surface-enhanced Raman spectroscopy of nonresonant molecules, *J. Am. Chem. Soc.* 131(40), 14466 (2009)
16. Y. Sawai, B. Takimoto, H. Nabika, K. Ajito, and K. Murakoshi, Observation of a small number of molecules at a metal nanogap arrayed on a solid surface using surface-enhanced Raman scattering, *J. Am. Chem. Soc.* 129(6), 1658 (2007)
17. S. L. Kleinman, E. Ringe, N. Valley, K. L. Wustholz, E. Phillips, K. A. Scheidt, G. C. Schatz, and R. P. Van Duyne, Single-molecule surface-enhanced Raman spectroscopy of crystal violet isotopologues: Theory and experiment, *J. Am. Chem. Soc.* 133(11), 4115 (2011)
18. K. Uosaki, H. Allen, and O. Hill, Absorption behaviour of 4,4′-bipyridyl at a gold/water interface and its role in the electron transfer reaction between cytochrome c and a gold electrode, *J. Electroanal. Chem. Interfacial Electrochem.* 122, 321 (1981)
19. D. Yang, D. Bizzotto, J. Lipkowski, B. Pettinger, and S. Mirwald, Electrochemical and second harmonic generation studies of 2,2'-bipyridine adsorption at the Au(111) electrode surface, *J. Phys. Chem.* 98(28), 7083 (1994)
20. H. Xu, J. Aizpurua, M. Käll, and P. Apell, Electromagnetic contributions to single-molecule sensitivity in surface-

enhanced Raman scattering, *Phys. Rev. E* 62(3), 4318 (2000)

21. A. J. Meixner, D. Zeisel, M. A. Bopp, and G. Tarrach, Superresolution imaging and detection of fluorescence from single molecules by scanning near-field optical microscopy, *Opt. Eng.* 34(8), 2324 (1995)
22. B. Pettinger, P. Schambach, C. J. Villagomez, and N. Scott, Tip-enhanced Raman spectroscopy: Near-fields acting on a few molecules, *Ann. Rev. Phys. Chem.* 63, 379 (2012)
23. J. Steidtner and B. Pettinger, Tip-enhanced Raman spectroscopy and microscopy on single dye molecules with 15 nm resolution, *Phys. Rev. Lett.* 100(23), 236101 (2008)
24. B. Pettinger, K. F. Domke, D. Zhang, G. Picardi, and R. Schuster, Tip-enhanced Raman scattering: Influence of the tip-surface geometry on optical resonance and enhancement, *Surf. Sci.* 603(10–12), 1335 (2009)
25. R. Zhang, Y. Zhang, Z. C. Dong, S. Jiang, C. Zhang, L. G. Chen, L. Zhang, Y. Liao, J. Aizpurua, Y. Luo, J. L. Yang, and J. G. Hou, Chemical mapping of a single molecule by plasmon-enhanced Raman scattering, *Nature* 498(7452), 82 (2013)
26. S. Berweger, C. C. Neacsu, Y. Mao, H. Zhou, S. S. Wong, and M. B. Raschke, Optical nanocrystallography with tip-enhanced phonon Raman spectroscopy, *Nat. Nanotechnol.* 4(8), 496 (2009)
27. Z. Liu, S. Y. Ding, Z. B. Chen, X. Wang, J. H. Tian, J. R. Anema, X. S. Zhou, D. Y. Wu, B. W. Mao, X. Xu, B. Ren, and Z. Q. Tian, Revealing the molecular structure of single-molecule junctions in different conductance states by fishing-mode tip-enhanced Raman spectroscopy, *Nat. Commun.* 2, 315 (2011)
28. T. Ichimura, S. Fujii, P. Verma, T. Yano, Y. Inouye, and S. Kawata, Subnanometric near-field Raman investigation in the vicinity of a metallic nanostructure, *Phys. Rev. Lett.* 102(18), 186101 (2009)
29. J. M. Klingsporn, M. D. Sonntag, T. Seideman, and R. P. Van Duyne, Tip-enhanced Raman spectroscopy with picosecond pulses, *J. Phys. Chem. Lett.* 5(1), 106 (2014)
30. J. M. Atkin and M. B. Raschke, Techniques: Optical spectroscopy goes intramolecular, *Nature* 498(7452), 44 (2013)
31. Y. Fang, Z. Zhang, L. Chen, and M. Sun, Near field plasmonic gradient effects on high vacuum tip-enhanced Raman spectroscopy, *Phys. Chem. Chem. Phys.* 17(2), 783 (2015)
32. L. Meng, Z. Yang, J. Chen, and M. Sun, Effect of electric field gradient on sub-nanometer spatial resolution of tip-enhanced Raman spectroscopy, *Sci. Rep.* 5, 9240 (2015)
33. P. Z. El-Khoury, Y. Gong, P. Abellan, B. W. Arey, A. G. Joly, D. Hu, J. E. Evans, N. D. Browning, and W. P. Hess, Tip-enhanced Raman nanographs: Mapping topography and local electric fields, *Nano Lett.* 15(4), 2385 (2015)
34. S. Kano, T. Tada, and Y. Majima, Nanoparticle characterization based on STM and STS, *Chem. Soc. Rev.* 44(4), 970 (2015)
35. S. V. Aradhya and L. Venkataraman, Single-molecule junctions beyond electronic transport, *Nat. Nanotechnol.* 8(6), 399 (2013)
36. I. Bâldea, Electrochemical setup — a unique chance to simultaneously control orbital energies and vibrational properties of single-molecule junctions with unprecedented efficiency, *Phys. Chem. Chem. Phys.* 16(47), 25942 (2014)
37. I. Baldea, Single-molecule junctions based on bipyridine: Impact of an unusual reorganization on charge transport, *J. Phys. Chem. C* 118(16), 8676 (2014)
38. F. Lissel, F. Schwarz, O. Blacque, H. Riel, E. Lörtscher, K. Venkatesan, and H. Berke, Organometallic single-molecule electronics: Tuning electron transport through $X(diphosphine)_2FeC_4Fe(diphosphine)_2X$ building blocks by varying the Fe-X-Au anchoring scheme from coordinative to covalent, *J. Am. Chem. Soc.* 136(41), 14560 (2014)
39. C. Huang, A. V. Rudnev, W. Hong, and T. Wandlowski, Break junction under electrochemical gating: Testbed for single-molecule electronics, *Chem. Soc. Rev.* 44(4), 889 (2015)
40. R. Matsuhita, M. Horikawa, Y. Naitoh, H. Nakamura, and M. Kiguchi, Conductance and SERS measurement of benzenedithiol molecules bridging between Au electrodes, *J. Phys. Chem. C* 117(4), 1791 (2013)
41. J. H. Tian, B. Liu, X. Li, Z. L. Yang, B. Ren, S. T. Wu, N. Tao, and Z. Q. Tian, Study of molecular junctions with a combined surface-enhanced Raman and mechanically controllable break junction method, *J. Am. Chem. Soc.* 128(46), 14748 (2006)
42. D. R. Ward, N. J. Halas, J. W. Ciszek, J. M. Tour, Y. Wu, P. Nordlander, and D. Natelson, Simultaneous measurements of electronic conduction and Raman response in molecular junctions, *Nano Lett.* 8(3), 919 (2008)
43. J. B. Herzog, M. W. Knight, Y. Li, K. M. Evans, N. J. Halas, and D. Natelson, Dark plasmons in hot spot generation and polarization in interelectrode nanoscale junctions, *Nano Lett.* 13(3), 1359 (2013)
44. T. Konishi, M. Kiguchi, M. Takase, F. Nagasawa, H. Nabika, K. Ikeda, K. Uosaki, K. Ueno, H. Misawa, and K. Murakoshi, Single molecule dynamics at a mechanically controllable break junction in solution at room temperature, *J. Am. Chem. Soc.* 135(3), 1009 (2013)
45. Y. Li, P. Doak, L. Kronik, J. B. Neaton, and D. Natelson, Voltage tuning of vibrational mode energies in single-molecule junctions, *Proc. Natl. Acad. Sci. USA* 111(4), 1282 (2014)
46. M. Kiguchi, T. Takahashi, M. Kanehara, T. Teranishi, and K. Murakoshi, Effect of end group position on the formation of single porphyrin molecular junction, *J. Phys. Chem. C* 113(21), 9014 (2009)
47. M. Kiguchi, S. Miura, T. Takahashi, K. Hara, M. Sawamura, and K. Murakoshi, Conductance of single 1,4-benzenediamine molecule bridging between Au and Pt electrodes, *J. Phys. Chem. C* 112(35), 13349 (2008)

48. M. Kiguchi, S. Miura, K. Hara, M. Sawamura, and K. Murakoshi, Conductance of single 1,4 di-substitued benzene molecules anchored to Pt electrodes, *Appl. Phys. Lett.* 91(5), 053110 (2007)
49. J. R. Lombardi, R. L. Birke, and G. Haran, Single molecule SERS spectral blinking and vibronic coupling, *J. Phys. Chem. C* 115(11), 4540 (2011)
50. P. K. Jain, D. Ghosh, R. Baer, E. Rabani, and A. P. Alivisatos, Near-field manipulation of spectroscopic selection rules on the nanoscale, *Proc. Natl. Acad. Sci. USA* 109(21), 8016 (2012)
51. A. M. Polubotko, Some anomalies of the SER spectra of symmetrical molecules adsorbed on transition metal substrates: Consideration by the dipole-quadrupole SERS theory, *J. Raman Spectrosc.* 36(6–7), 522 (2005)
52. D. V. Chulhai, and L. Jensen, Determining molecular orientation with surface-enhanced Raman scattering using inhomogenous electric fields, *J. Phys. Chem. C* 117, 19622 (2013)
53. E. J. Ayars, H. D. Hallen, and C. L. Jahncke, Electric field gradient effects in Raman spectroscopy, *Phys. Rev. Lett.* 85(19), 4180 (2000)
54. G. S. Duesberg, I. Loa, M. Burghard, K. Syassen, and S. Roth, Polarized raman spectroscopy on isolated single-wall carbon nanotubes, *Phys. Rev. Lett.* 85(25), 5436 (2000)
55. K. Kneipp, A. Jorio, H. Kneipp, S. D. M. Brown, K. Shafer, J. Motz, R. Saito, G. Dresselhaus, and M. S. Dresselhaus, Polarization effects in surface-enhanced resonant Raman scattering of single-wall carbon nanotubes on colloidal silver clusters, *Phys. Rev. B* 63, 081401 (2001)
56. A. Jorio, M. A. Pimenta, A. G. Souza Filho, G. G. Samsonidze, A. K. Swan, M. S. Unlü, B. B. Goldberg, R. Saito, G. Dresselhaus, and M. S. Dresselhaus, Resonance Raman spectra of carbon nanotubes by cross-polarized light, *Phys. Rev. Lett.* 90(10), 107403 (2003)
57. N. Hayazawa, T. Yano, H. Watanabe, Y. Inouye, and S. Kawata, Detection of an individual single-wall carbon nanotube by tip-enhanced near-field Raman spectroscopy, *Chem. Phys. Lett.* 376(1–2), 174 (2003)
58. A. Hartschuh, E. J. Sánchez, X. S. Xie, and L. Novotny, High-resolution near-field Raman microscopy of single-walled carbon nanotubes, *Phys. Rev. Lett.* 90(9), 095503 (2003)
59. M. Takase, H. Ajiki, Y. Mizumoto, K. Komeda, M. Nara, H. Nabika, S. Yasuda, H. Ishihara, and K. Murakoshi, Selection-rule breakdown in plasmon-induced electronic excitation of an isolated single-walled carbon nanotube, *Nat. Photonics* 7, 550 (2013)
60. C. M. Aikens, L. R. Madison, and G. C. Schatz, Raman Spectroscopy: The effect of field gradient on SERS, *Nat. Photonics* 7(7), 508 (2013)
61. S. Heeg, A. Oikonomou, R. Fernandez-Garcia, C. Lehmann, S. A. Maier, A. Vijayaraghavan, and S. Reich, Plasmon-enhanced Raman scattering by carbon nanotubes optically coupled with near-field cavities, *Nano Lett.* 14(4), 1762 (2014)
62. M. T. Trinh, M. Y. Sfeir, J. J. Choi, J. S. Owen, and X. Zhu, A hot electron-hole pair breaks the symmetry of a semiconductor quantum dot, *Nano Lett.* 13(12), 6091 (2013)
63. M. S. Tame, K. R. McEnery, Ş K. Özdemir, J. Lee, S. A. Maier, and M. S. Kim, Quantum plasmonics, *Nat. Phys.* 9(6), 329 (2013)
64. M. Barbry, P. Koval, F. Marchesin, R. Esteban, A. G. Borisov, J. Aizpurua, and D. Sánchez-Portal, Atomistic near-field nanoplasmonics: Reaching atomic-scale resolution in nanooptics, *Nano Lett.* 15(5), 3410 (2015)
65. K. J. Savage, M. M. Hawkeye, R. Esteban, A. G. Borisov, J. Aizpurua, and J. J. Baumberg, Revealing the quantum regime in tunnelling plasmonics, *Nature* 491(7425), 574 (2012)
66. A. Manjavacas, F. J. García de Abajo, and P. Nordlander, Quantum plexcitonics: Strongly interacting plasmons and excitons, *Nano Lett.* 11(6), 2318 (2011)
67. P. Törmä and W. L. Barnes, Strong coupling between surface plasmon polaritons and emitters: A review, *Rep. Prog. Phys.* 78(1), 013901 (2015)